



HAL
open science

Multivariate classification provides a neural signature of Tourette disorder

Giuseppe A Zito, Andreas Hartmann, Benoît Béranger, Samantha Weber, Selma Aybek, Johann Faouzi, Emmanuel Roze, Marie Vidailhet, Yulia Worbe

► **To cite this version:**

Giuseppe A Zito, Andreas Hartmann, Benoît Béranger, Samantha Weber, Selma Aybek, et al.. Multivariate classification provides a neural signature of Tourette disorder: Running head: Multivariate analysis of Tourette disorder. *Psychological Medicine*, 2021. hal-03480739

HAL Id: hal-03480739

<https://inria.hal.science/hal-03480739>

Submitted on 15 Dec 2021

HAL is a multi-disciplinary open access archive for the deposit and dissemination of scientific research documents, whether they are published or not. The documents may come from teaching and research institutions in France or abroad, or from public or private research centers.

L'archive ouverte pluridisciplinaire **HAL**, est destinée au dépôt et à la diffusion de documents scientifiques de niveau recherche, publiés ou non, émanant des établissements d'enseignement et de recherche français ou étrangers, des laboratoires publics ou privés.

1 **Title:** Multivariate classification provides a neural signature
2 of Tourette disorder

3 **Running head:** Multivariate analysis of Tourette disorder

4 Giuseppe A. Zito, PhD^{1,2}, Andreas Hartmann, MD^{1,3}, Benoît Béranger, MSc⁴, Samantha Weber,
5 MSc⁵, Selma Aybek, MD⁵, Johann Faouzi, MSc⁶, Emmanuel Roze, MD PhD¹, Marie Vidailhet,
6 MD¹ and Yulia Worbe, MD, PhD^{1,3,7*}

7
8 ¹ Sorbonne University, Inserm U1127, CNRS UMR7225, UM75, Paris Brain Institute, Movement
9 Investigation and Therapeutics Team, Paris, FR

10 ² Support Centre for Advanced Neuroimaging (SCAN), University Institute of Diagnostic and
11 Interventional Neuroradiology, Inselspital, Bern University Hospital, University of Bern,
12 Freiburgstrasse, Bern, CH-3010, CH

13 ³ National Reference Center for Tourette Syndrome, Assistance Publique-Hôpitaux de Paris,
14 Groupe Hospitalier Pitié-Salpêtrière, Paris, FR

15 ⁴ Center for Neuroimaging Research (CENIR), Paris Brain Institute, Sorbonne University, UPMC
16 Univ Paris 06, Inserm U1127, CNRS UMR 7225, Paris, France

17 ⁵ Psychosomatics Unit of the Department of Neurology, Inselspital, Bern University Hospital,
18 University of Bern, Freiburgstrasse, Bern, CH-3010, CH

19 ⁶ Sorbonne University, Inserm U1127, CNRS UMR7225, UM75, ICM, Inria Paris, Aramis project-
20 team, Paris, FR

21 ⁷ Department of Neurophysiology, Saint-Antoine Hospital, Assistance Publique - Hôpitaux de
22 Paris, Paris, FR

23

24 *** Corresponding author:**

25 Dr. Yulia Worbe
26 Paris Brain Institute (ICM), Movement Investigation and Therapeutics Team
27 University Hospitals Pitié Salpêtrière - Charles Foix, 47-83 Boulevard de l'Hôpital, 75013
28 Paris, FR
29 Tel: +33 (0)1 42161316
30 E-mail: yulia.worbe@aphp.fr

31

32 **Word count:** 4142

33 **ABSTRACT**

34

35 **Background:**

36 Tourette disorder (TD), hallmarks of which are motor and vocal tics, has been related to functional
37 abnormalities in large-scale brain networks. Using a fully-data driven approach in a prospective,
38 case-control study, we tested the hypothesis that functional connectivity of these networks carries
39 a neural signature of TD. Our aim was to investigate (i) the brain networks that distinguish adult
40 patients with TD from controls, and (ii) the effects of antipsychotic medication on these networks.

41 **Methods:**

42 Using a multivariate analysis based on support vector machine (SVM), we developed a predictive
43 model of resting state functional connectivity in 48 patients and 51 controls, and identified brain
44 networks that were most affected by disease and pharmacological treatments. We also performed
45 standard univariate analyses to identify differences in specific connections across groups.

46 **Results:**

47 SVM was able to identify TD with 67% accuracy ($p=0.004$), based on the connectivity in
48 widespread networks involving the striatum, fronto-parietal cortical areas and the cerebellum.
49 Medicated and unmedicated patients were discriminated with 69% accuracy ($p=0.019$), based on
50 the connectivity among striatum, insular and cerebellar networks. Univariate approaches revealed
51 differences in functional connectivity within the striatum in patients vs. controls, and between the
52 caudate and insular cortex in medicated vs. unmedicated TD.

53 **Conclusions:**

54 SVM was able to identify a neuronal network that distinguishes patients with TD from control, as
55 well as medicated and unmedicated patients with TD, holding a promise to identify imaging-based
56 biomarkers of TD for clinical use and evaluation of the effects of treatment.

57

58

59 **INTRODUCTION**

60 Tourette disorder (TD) is a neurodevelopmental disorder characterized by motor and vocal tics
61 (Association, 2013). It is often associated with psychiatric comorbidities, of which obsessive–
62 compulsive disorders (OCD), attention-deficit hyperactivity disorders (ADHD), intermittent
63 explosive disorders (IED) and depression represent the most common ones (Hirschtritt et al.,
64 2015).

65 A dysfunction of cortico-striato-thalamo-cortical (CSTC) loops might account for this clinical
66 spectrum (Singer, 2005), as structural and functional abnormalities have been found in the basal
67 ganglia (Worbe et al., 2010; Worbe et al., 2012), the sensory-motor areas (Fahim et al., 2010;
68 Worbe et al., 2010), the dorsolateral prefrontal cortex and more generally the frontal cortex
69 (Fredericksen et al., 2002; Kates et al., 2002), fronto-parietal networks (Atkinson-Clement et al.,
70 2020; Eddy, Cavanna, Rickards, & Hansen, 2016) and the cerebellum (Lerner et al., 2007). Some
71 of these abnormalities have been related to the disorder itself, but others have been associated
72 with comorbidities, as well as with compensatory strategies to reduce the tics (Mazzone et al.,
73 2010). Despite an extensive research, no reliable brain biomarker of this disorder has been found,
74 and the precise pathophysiological mechanisms of TD are still poorly understood.

75 Multivariate approaches applied to neuroimaging, such as functional magnetic resonance imaging
76 (fMRI), represent a valuable method to address the complex aspects of TD, due to their ability to
77 (i) detect subtle and distributed patterns of activity throughout the brain in a fully data-driven
78 manner, (ii) make predictions that have the potential to interrogate neurophysiological
79 mechanisms, and (iii) aid in diagnosis and treatment (Nielsen, Barch, Petersen, Schlaggar, &
80 Greene, 2019). Recent studies have used multivariate approaches, in particular support vector
81 machine (SVM), to discriminate children with TD from age-matched healthy controls (HC)
82 (Greene et al., 2016), as well as young TD patients from older ones (Nielsen et al., 2020). They
83 have shown that functional brain abnormalities allow for the identification of TD with ~70%
84 accuracy, and that delayed brain maturation may explain the atypical functional connectivity in
85 adults with TD. However, they did not search a neural signature of the disorder in relation to

86 pharmacological treatment. This is relevant, as patients with TD are often treated with
87 antipsychotics and, even if their effects on the symptoms are documented, their specific action on
88 large-scale brain networks are still unknown (Handley et al., 2013).

89 We employed a multivariate approach to predict patterns of resting state functional connectivity
90 (rs-FC) in TD which: (i) inform on the neurophysiological mechanisms of adult TD, (ii) address the
91 differences between TD patients under antipsychotic medication and unmedicated ones and (iii)
92 correlate with symptoms' severity. We applied SVM to identify differences in connectivity patterns
93 between TD patients and HC, as well as between patients with and without medication. We also
94 implemented a support vector regression (SVR) model that investigates whether rs-FC carries
95 information about symptoms' severity. In addition to SVM, we performed a standard univariate
96 analysis to evaluate specific differences in rs-FC across groups.

97 Our ultimate goal was to shed light on the altered brain functions underpinning TD in adults, as
98 well as their link to medication status, and to study the potential of SVM as predictive tool to
99 support the diagnosis of TD.

100

101 **MATERIALS AND METHODS**

102 ***Participants and general procedure***

103 We recruited 55 patients with TD and 55 sex- and age-matched HC. Seven patients and four HC
104 were not able to perform the MRI (due to e.g., excessive movements) and were excluded from the
105 analysis. The final sample consisted of 48 patients with TD (39 male, mean age: 30.5 ± 10.3 years)
106 and 51 HC (33 male, mean age: 30.9 ± 10.4 years).

107 Patients were recruited through the National Tourette Disorder reference center at the Pitié-
108 Salpêtrière Hospital in Paris. Inclusion criteria for patients were: a diagnosis of TD according to
109 the DSM-5 (Association, 2013), capability to control tics for at least 10 minutes during the MRI
110 acquisition. Exclusion criteria for both HC and patients with TD were: incompatibility with MR
111 acquisition (e.g., claustrophobia, metallic body implants), history of alcohol or drug addiction
112 (excepted nicotine and recreational cannabis use for less than once per week), history of

113 psychosis and learning disability. We also excluded HC who experienced childhood tics and any
114 neurological disorders.

115 In patients, tic severity was assessed using the Yale Global Tic Severity Scale (YGTSS50)
116 (Leckman et al., 1989). The life-long diagnosis of psychiatric comorbidities, such as obsessive–
117 compulsive disorders (OCD), attention-deficit hyperactivity disorders (ADHD), and intermittent
118 explosive disorders (IED), typically observed in TD (Hirschtritt et al., 2015), was evaluated using
119 patients' medical records and psychiatric evaluations available at the inclusion in the study.
120 Eighteen patients with TD were under stable medication for at least three years at the time of
121 examination (Table 1).

122 ***Standard Protocol Approvals, Registrations and Patients Consent***

123 The study was carried out in accordance with the latest version of the Declaration of Helsinki and
124 approved by the local Ethics Committee (approval number: CCP16163/C16-07). All participants
125 gave written informed consent prior to the study. The study was registered in ClinicalTrials.gov (ID
126 number: NCT02960698).

127 ***Clinical groups' analysis***

128 We performed two analyses investigating: (i) between-group differences in 51 HC and 48 patients
129 with TD, and (ii) between-TD patients' subgroup differences in 18 patients with medication and 18
130 patients without medication. For the latter, as SVM achieves best performance when the two
131 discriminated groups contain the same number of samples (Wu & Chang, 2003), we analyzed
132 data from all patients with TD under medication ($n = 18$) and a subset of 18 unmedicated patients
133 that matched the group of medicated TD for age, sex, symptom severity and comorbidities. This
134 ensured balanced groups, and excluded potential confounds due to between-group differences
135 other than in rs-FC.

136 Differences in age were assessed with independent-sample t-tests, whereas differences in the
137 ratio between male and female participants were assessed with χ^2 tests. Moreover, for the
138 between-TD patients' subgroup analysis, differences in the YGTSS50 were assessed with
139 independent-sample t-tests, and differences in the ratio of patients with and without IED, ADHD

140 and OCD were assessed with χ^2 tests. The significance level was set at 0.05. Data analysis was
141 performed with SPSS 25 (IBM Statistics, USA).

142 ***Neuroimaging acquisition parameters and pre-processing***

143 During the MR session, participants were asked to lie still with the eyes open, while fixating a
144 cross on a screen. Eye movements were monitored with an eye-tracking device. Neuroimaging
145 data were acquired using a 3T Magnetom Prisma (Siemens, DE) with a 64-channel head coil.

146 Resting state fMRI and structural images were acquired in one session using the following
147 parameters: (i) echo-planar imaging (EPI) sequences performed with a multi-slice, multi-echo
148 acquisition, Repetition Time (TR)=1.9 s, Echo Time (TE)=17.2/36.62/56.04 ms, lpat acceleration
149 factor=2, Multi-band=2, isotropic voxel size=3 mm, dimensions=66x66 in plane x46 slices, 350
150 volumes, duration=11 min; (ii) a T1-weighted MP2RAGE sequence with TR=5 s, Inversion Time
151 (TI)=700/2500 ms, field of view (FOV)=232x256 in plane x176 slices, 1 mm isotropic, lpat
152 acceleration factor=3.

153 T1-weighted images were first background denoised (O'Brien et al., 2014) using
154 <https://github.com/benoitberanger/mp2rage>, which is based on (Marques). This step improved the
155 quality of the subsequent segmentation. Images were then pre-processed (segmentation,
156 normalisation to Montreal Neurological Institute – MNI – space) using the Computational Anatomy
157 Toolbox (<http://www.neuro.uni-jena.de/cat/>) extension for SPM12
158 (<https://www.fil.ion.ucl.ac.uk/spm/>).

159 Functional data were pre-processed with AFNI using *afni_proc.py* script
160 (<https://afni.nimh.nih.gov/>) according to standard procedures (despiking, slice timing correction
161 and realignment to the volume with the minimum outlier fraction driven by the first echo). A brain
162 mask was computed on the realigned shortest echo temporal mean using FSL BET (Jenkinson,
163 Beckmann, Behrens, Woolrich, & Smith, 2012). This step increased the robustness against strong
164 signal bias intensity. Afterwards, the TEDANA toolbox (Kundu et al., 2017) version 0.0.7 was
165 used to optimally combine the realigned echoes, to reduce the dimensionality of the dataset by
166 applying principal component analysis, and to perform an independent component analysis (ICA)

167 decomposition which separated BOLD from non-BOLD components, based on the echo time
168 dependence of the ICA components (Kundu, Inati, Evans, Luh, & Bandettini, 2012). This step
169 ensured robust artefact removal of non-BOLD components, such as movement, respiration or
170 heartbeat. Previous research with resting state fMRI has already confirmed the superiority of this
171 method in regressing out motion over standard denoising techniques (Kundu et al., 2017). To
172 further confirm this, Framewise displacement (FD) was computed according to standard methods
173 (Power et al., 2014), and compared between the groups. No motion artefacts affected the quality
174 of the signal, the FD in TD (0.016 ± 0.007 mm) did not statistically differ from HC (0.136 ± 0.006
175 mm) [$t(97)=1.91$, $p=0.059$], and FD in patients with medication (0.016 ± 0.009 mm) did not
176 statistically differ from patients without medication (0.016 ± 0.005 mm) [$t(34)=0.21$, $p=0.830$].
177 Finally, using SPM12, images were co-registered to the anatomical scan, normalized to MNI
178 space, then smoothed with a Gaussian kernel with full width at half maximum of $5\times 5\times 5$ mm.
179 Brain images were parcellated into 116 functional regions, based on the Automatic Anatomical
180 Labelling (AAL) Atlas (Tzourio-Mazoyer et al., 2002), and the region-averaged time series were
181 extracted. The first 10 time points were discarded to ensure magnetization equilibrium. Motion
182 parameters and the average signal of white matter and cerebrospinal fluid obtained during the
183 segmentation, were regressed out. Time series were finally band-pass filtered at $0.009 < f < 0.08$
184 Hz, according to previous studies (Greene et al., 2016; Nielsen et al., 2020). We computed
185 pairwise Pearson correlation coefficients between all pairs of brain regions as indicators of their
186 functional connectivity, and we obtained a symmetric correlation matrix of 116×116 coefficients for
187 each participant, i.e., 6670 correlation coefficients. Next, we converted the correlation coefficients
188 to z-scores using Fisher-Z transformation, in order to normalize them to a Gaussian distribution
189 (Wegrzyk et al., 2018).

190 ***Multivariate analysis for neuroimaging data***

191 The 6670 correlation coefficients were used as features for linear SVM models. We implemented
192 three predictive models to: (i) distinguish HC from patients with TD, (ii) distinguish patients with
193 and without medication and (iii) predict symptoms' severity in patients with TD. The first two

194 models were initially optimized with an automatic grid search algorithm based on Bayesian
195 Optimization (Hastie, Tibshirani, & Friedman, 2009). The optimization minimized the cross-
196 validation loss (error) by iteratively varying the C parameter and Kernel Scale. In line with
197 previous research (Nielsen et al., 2020; Wegrzyk et al., 2018), the best values were found to be
198 $C=1$ and Kernel Scale=1. The models were then trained to learn a function that separates the two
199 groups, based on the differences in their rs-FC. The models were trained on a known dataset of
200 participants belonging to the two groups, and mathematically assigned weights to each
201 connection, based on its contribution to the discrimination. Once the models were built, they used
202 these weights to predict the group where a new and unknown participant belongs to. We applied
203 leave-one-subject-out-cross-validation (LOSOCV) to estimate the generalization of the models.
204 The statistical significance of the classification accuracy was assessed using its null distribution
205 under permutation testing, where group labels were randomly permuted 1000 times. We finally
206 trained the SVMs with all HC and patients, and identified the most discriminative connections as
207 the ones holding the highest weights (Wegrzyk et al., 2018). This step was performed after
208 evaluating that the most discriminative connections obtained following training the SVM with the
209 entire dataset were consistent with the ones calculated by the single LOSOCV folds
210 (Supplementary Figure 1). We studied whether rs-FC contains information about symptom
211 severity by implementing a SVR model ($C=\infty$, Kernel Scale=1, $\epsilon=0.00001$, according to previous
212 research (Nielsen et al., 2020) and optimized with Bayesian Optimization, as described above) to
213 predict YGTSS50 (Greene et al., 2016), and estimated it with LOSOCV. We studied the
214 performance of the SVR model with r^2 . The SVM and SVR were implemented with the Statistics
215 and Machine Learning Toolbox in Matlab R2018a (The MathWorks, USA).

216 ***Univariate analysis for neuroimaging data***

217 We performed a standard univariate analysis to study specific differences in rs-FC across groups.
218 We compared the 6670 correlation coefficients between HC and patients with TD, and between
219 patients with and without medication, respectively, with multiple independent t-tests. Moreover, in
220 patients with TD, we computed Pearson's correlation coefficients between each connection and

221 the YGTSS50. All tests were corrected for multiple comparisons with 1000 permutations. The
222 significance level was set to 0.05 after correction. Data analysis was implemented in Matlab
223 R2018a.

224

225 **RESULTS**

226 ***Subjects***

227 No statistically significant differences were found in sex and age between TD and HC. No
228 statistically significant differences were found in tic severity and in the occurrence of comorbidities
229 between medicated and unmedicated patients. Demographic and clinical data are presented in
230 Table 1.

231 *Table 1 about here*

232

233 ***Multivariate analysis of resting state functional connectivity between the groups***

234 The performance of the first two classifiers is shown in Table 2. The classifiers discriminated TD
235 from HC ($p=0.004$), as well as TD with and without medication ($p=0.019$), with accuracy,
236 specificity and sensitivity well above chance.

237 *Table 2 about here*

238 For the between-group classification analysis, the SVM identified the most discriminative
239 connections, i.e., the connections holding the highest weights, in fronto-cerebellar, fronto-parietal,
240 parieto-cerebellar and subcortico-subcortical networks (Figure 1A and Supplementary Figure 1A).
241 In particular, Figure 1A shows that the classification accuracy was driven by the connectivity
242 between (i) the cerebellar lobule 7b and the superior parietal gyrus, (ii) the orbito-frontal cortex
243 (OFC) and the angular gyrus, (iii) the putamen and the caudate, (iv) the caudate and the
244 cerebellar lobule 10, and (v) the cerebellar vermis 9 and the OFC (Supplementary Table 1).

245 For the between-TD patients' subgroup classification analysis, the SVM identified the most
246 discriminative connections in fronto-cerebellar, cerebello-limbic, parieto-cerebellar and cerebello-
247 subcortical networks (Figure 1B and Supplementary Figure 1B). Figure 1B shows that the
248 performance of the classifier was driven by the connectivity (i) of the supplementary motor area
249 (SMA) with the cerebellar lobule 7b and the supramarginal gyrus, respectively, (ii) within the
250 cerebellar regions, namely between crus 2 and, respectively, 4th, 5th, and 10th lobules, (iii)
251 between the right caudate and the right insula, and (iv) between the cerebellum (vermis 9 and 9th
252 lobule) and the OFC and the inferior frontal gyrus (IFG), respectively (Supplementary Table 2).
253 These patterns were independent of the number of top feature weights considered, as shown in
254 Supplementary Figure 2.
255 The analysis of the SVR showed that rs-FC was not able to predict symptom severity in patients
256 with TD ($r^2=0.05$, $p=0.114$).

257 *Figure 1 about here*

258

259 ***Univariate analysis of resting state functional connectivity***

260 The univariate analysis showed increased functional connectivity, in patients with TD compared to
261 HC (Figure 2A), of the right caudate with the right and left putamen, respectively [$t(97)=5.06$,
262 $p_{\text{corrected}}=0.003$ and $t(97)=5.29$, $p_{\text{corrected}}=0.001$], and of the left caudate with the right and left
263 putamen, respectively [$t(97)=4.21$, $p_{\text{corrected}}=0.050$ and $t(97)=4.38$, $p_{\text{corrected}}=0.037$].

264 In the between-TD patients' subgroup analysis, the connectivity between the right caudate and
265 the right insula was lower in medicated vs. unmedicated patients [$t(34)=4.77$, $p_{\text{corrected}}=0.050$]
266 (Figure 2B).

267 No correlation between YGTSS50 and any of the connections was found in patients with TD
268 ($p_{\text{corrected}}>0.05$).

269 *Figure 2 about here*

270

271 **DISCUSSION**

272 Using rs-FC and a multivariate approach in a fully data-driven manner, we were able to
273 significantly discriminate adult patients with TD from HC, and patients with and without
274 medication. Compared to HC, patients with TD showed abnormal rs-FC among widespread brain
275 areas, including striatum and cerebellum. Functional connectivity of the SMA, the OFC, the insula
276 and the posterior parietal cortex, as well as the striatum and the cerebellum discriminated the
277 patients under conventional medication with antipsychotics, such as aripiprazole (APZ), from the
278 unmedicated patients. The univariate analysis found significant differences in connectivity
279 between HC and patients with TD within the striatum, and between medicated and unmedicated
280 patients with TD in the connection between the caudate nucleus and the insula.

281 Our study has some limitations. First, we chose the AAL atlas based on existing literature on
282 classification of rs-FC using a similar pipeline as in our study (Lee & Frangou, 2017; Richiardi et
283 al., 2012; Wegrzyk et al., 2018). The choice of the atlas was crucial for our approach, as the brain
284 parcellation might have a major impact on the definition of the regions of interest, hence on the
285 connectivity patterns, and ultimately on the results. However, previous research has compared
286 the rs-FC classification performance across different atlases (Wegrzyk et al., 2018), and found
287 similar accuracy of ~70% when using, for instance, the AAL, the Hammers (Hammers et al.,
288 2003) and the Shirer (Shirer, Ryali, Rykhlevskaia, Menon, & Greicius, 2012) atlases. Second, we
289 compared the medicated and non-medicated patients with TD in a parallel design. It is possible
290 that patients under medication have substantial differences from the group of unmedicated
291 patients. Thus, to fully address the question of APZ effect on brain networks, the same patients
292 with TD should be assessed before and after the beginning of pharmacological treatment.

293 Overall, our results strengthen previous knowledge of altered brain networks in adult TD, and
294 provide new evidence of specific patterns of functional connectivity in TD patients with
295 pharmacological treatment.

296 ***Differences in functional connectivity between TD and controls***

297 The results indicated large-scale networks' alteration in adult TD, and specifically in the
298 connectivity between cortical areas, the cerebellum and the striatum. Other studies in patients
299 with TD have confirmed functional and structural abnormalities between the striatum and sensory-
300 motor cortices, OFC, parietal and temporal regions, similar to our results (Martino, Ganos, &
301 Worbe, 2018).

302 The connectivity within the striatum was among the most discriminative features of our
303 multivariate analysis. This structure, as central part of the CSTC network (Singer, 2005; Worbe,
304 Lehericy, & Hartmann, 2015), has been suggested by various animal models to account for the
305 wide spectrum of TD symptoms (Bronfeld, Yael, Belevovsky, & Bar-Gad, 2013; Worbe et al.,
306 2013). Recent computational models of pathophysiology of TD have also suggested that tics and
307 premonitory urges result from the abnormal computation of the sensation and action within
308 sensory-motor regions of the striatum (Rae, Critchley, & Seth, 2019).

309 The connectivity of cerebello-cortical and cerebello-cerebellar networks was also among the most
310 discriminative features of patients with TD compared to HC. These results are in line with data
311 obtained from animal models of TD, suggesting that tics result from the global neuronal rhythms
312 abnormalities of cerebro-basal ganglia-cerebellar networks, due to striatal disinhibition (McCairn,
313 Iriki, & Isoda, 2013). In particular, there is evidence that a cerebellar-prefrontal network is
314 implicated in motor execution specific to Go events in Go-no-Go tasks (Mostofsky et al., 2003),
315 and our results showed an impairment in such a network, which may lead to an alteration of
316 unwanted movement suppression and, in turn, to tic release. Numerous studies have further
317 confirmed abnormal structural and functional connectivity of the cerebellum with cortical areas
318 and basal ganglia, namely the striatum (Ramkiran, Heidemeyer, Gaebler, Shah, & Neuner, 2019;
319 Sigurdsson, Jackson, Jolley, Mitchell, & Jackson, 2020) in patients with TD.

320 Overall, our results point to the pivotal role of the striatum and cerebellum in the pathophysiology
321 of TD. They also suggest that functional connectivity of the striatum, cerebello-cerebellar and
322 cerebello-cortical networks might be considered as potential imaging biomarkers of this disorder.
323 However, and similar to previous research (Greene et al., 2016), SVR was not able to predict tic
324 severity. This could result from the fact that only patients with low-to-moderate tic severity were

325 included in the study, to guarantee the quality of MRI acquisitions. Further studies combining
326 structural and functional connectivity are warranted to address this question. For instance, a
327 larger hippocampal volume in children with TD predicted the persistence of tics in follow up visits
328 after onset (Sigurdsson et al., 2020). Moreover, our sample did not allow us to study the effects of
329 comorbid disorders on rs-FC. Future research with a large number of patients will allow for the
330 stratification of TD according to comorbidities, in order to disentangle their contribution to
331 networks dysfunction. One potential limitation of this study is that we included only patients with
332 low-to-moderate tics that did not impact the quality of the images. Also, even if the patients were
333 not explicitly instructed to suppress their tics, some of them might have still performed this
334 voluntary suppression, and this could have had an impact on the results.

335 ***Differences in functional connectivity between medicated and unmedicated TD***

336 The most common drug used to treat TD in this study was APZ, taken by 83% of medicated
337 patients. This antipsychotic acts on the dopaminergic and serotonergic function as a partial
338 agonist of the dopamine D2 receptor and 5-HT1A, and antagonism at 5-HT2A receptors (Jordan
339 et al., 2004). It has shown a positive effect on tics in TD (Bubl, Perlov, & Tebartz Van Elst, 2006;
340 Kastrup, Schlotter, Plewnia, & Bartels, 2005).

341 The empirical model of APZ action postulates that brain areas with high density of neurons with
342 dopamine D2 receptors (D2R) might be more sensitive to this drug, and might in turn influence
343 the activity of other regions innervated by the D2R neurons (Handley et al., 2013). Previous
344 research has shown that, compared to placebo, APZ intake in healthy volunteers modulates
345 activity in a network including the putamen, the insula, the caudate and the cerebellum, as well as
346 in the superior frontal gyrus, the superior and inferior parietal lobes and the OFC (Handley et al.,
347 2013), all regions found discriminative of medicated compared to unmediated patients in the
348 present study. The univariate approach pointed to differences in the connectivity between the
349 caudate and the insula in medicated compared to unmedicated patients. The insula has been
350 related to the “urge-for-action” (Worbe et al., 2015), i.e., suppression of natural urges (such as
351 blinking), in healthy participants (Lerner et al., 2009), but also to uncomfortable feeling associated

352 with the premonitory urges in TD (Jackson, Parkinson, Kim, Schüermann, & Eickhoff, 2011). In
353 particular, a brain network encompassing the insular cortex has been found active prior to tic
354 onset, and concomitant with the subjective experience of the premonitory urge (Bohlhalter et al.,
355 2006). Similarly, functional connectivity (Tinaz, Malone, Hallett, & Horovitz, 2015) and cortical
356 thickness (Draper, Jackson, Morgan, & Jackson, 2016) of the insula have been correlated with
357 the urge to tic in TD. Altogether, these findings support a key role of the insula in the perception of
358 bodily urges, linking the sensory and emotional character of premonitory urges with their
359 translation into tics (Cavanna, Black, Hallett, & Voon, 2017; Conceição, Dias, Farinha, & Maia,
360 2017; Cox, Seri, & Cavanna, 2018). In this study we have not monitored premonitory urges in
361 patients with TD, however, our results indicate that antipsychotics might act on insular and striatal
362 loops, and the tics improvement might result from premonitory urges reduction. This points to a
363 potential effect of APZ on striatal, insular, and cerebellar networks, and the activity of these areas
364 might be used in future research to monitor the effects of medication.

365 One potential confound is the use of concomitant medications other than APZ, which may have
366 an impact on rs-FC. Due to our sample size, we did not stratify according to medication type,
367 however, most of our patients was under APZ, and our findings are in line with existing evidence
368 of altered cortical and subcortical activity in healthy participants after APZ (Handley et al., 2013).
369 It is therefore unlikely that the other drugs biased our predictions.

370 Overall, these results suggest that antipsychotic medication might affect the activity of areas
371 within the CSTC loop implicated in tic generation and volitional control (Ganos, Roessner, &
372 Münchau, 2013). Its benefic effects on these areas may in turn spread to other regions
373 functionally connected to the CSTC loop, and improve other cognitive functions impaired in TD.

374 ***Advantages of multivariate approaches***

375 The results of our study demonstrated that multivariate approaches can be successfully used to
376 predict adult TD based on abnormal patterns of rs-FC. Recent studies have confirmed the
377 advantage of multivariate approaches, in particular SVM, in investigating patterns of differential
378 functional connectivity between children and adults with TD (Nielsen et al., 2020), or between

379 children with TD and age-matched HC (Greene et al., 2016). Yet, these studies have applied a
380 feature reduction, and restricted the analysis to a smaller number of connections (Greene et al.,
381 2016). Indeed, this methodological choice improves the classification accuracy and computational
382 time, as the complexity of the model is reduced, however, it introduces *a priori* information on
383 which regions carry the relevant information, often achieved through univariate comparisons
384 (Greene et al., 2016), and might thus exclude other areas still relevant for the understanding of
385 TD. Moreover, the interpretability of the results obtained after feature selection has been recently
386 questioned (Nielsen et al., 2019). We opted for no feature selection, as we were interested in the
387 connectivity at the whole-brain scale, and our classifier showed similar performance to other
388 studies in TD (Greene et al., 2016; Nielsen et al., 2020).

389 **CONCLUSIONS**

390 Overall, our results showed the potential of multivariate classification methods for clinical use, to
391 help the diagnostic process and/or to evaluate the effects of treatments. Also, the results of this
392 study hold a promise to identify an imaging-based biomarker of TD and to monitor treatments.
393 Future research on a larger sample will allow for accurate models in relationship with co-
394 morbidities of TD, and will move the field closer towards imaging-based biomarkers to guide
395 clinical decisions (Wolfers, Buitelaar, Beckmann, Franke, & Marquand, 2015).

396 **ACKNOWLEDGEMENTS**

397 The Authors would like to acknowledge the Swiss National Science Foundation (SNSF), the Paris
398 Brain Institute, and the University Hospitals Pitié-Salpêtrière for the support. We would also like to
399 thank all the participants of our study.

400 **FINANCIAL SUPPORT**

401 This work was supported by the Swiss National Science Foundation (GAZ, grant
402 P400PM_183958), the Fondation pour la Recherche Médicale (FRM), the French association for

403 Tourette disorder (AFSGT) and the National Research Agency (YW, grant ANR-18-CE37-0008-
404 01).

405 **CONFLICT OF INTEREST**

406 None.

407 **ETHICAL STANDARDS**

408 The authors assert that all procedures contributing to this work comply with the ethical standards
409 of the relevant national and institutional committees on human experimentation and with the
410 Helsinki Declaration of 1975, as revised in 2008.

411 **REFERENCES**

- 412 American Psychological Association, A. P. (2013). *Diagnostic and statistical manual of mental*
413 *disorders (DSM-5®)*: American Psychiatric Pub.
- 414 Atkinson-Clement, C., Porte, C.-A., de Liege, A., Wattiez, N., Klein, Y., Beranger, B., . . . Pouget,
415 P. (2020). Neural correlates and role of medication in reactive motor impulsivity in
416 Tourette disorder. *Cortex*, 125, 60-72.
- 417 Beranger, B. Retrieved from <https://github.com/benoitberanger/mp2rage>
- 418 Bohlhalter, S., Goldfine, A., Matteson, S., Garraux, G., Hanakawa, T., Kansaku, K., . . . Hallett, M.
419 (2006). Neural correlates of tic generation in Tourette syndrome: an event-related
420 functional MRI study. *Brain*, 129(8), 2029-2037.
- 421 Bronfeld, M., Yael, D., Belevovsky, K., & Bar-Gad, I. (2013). Motor tics evoked by striatal
422 disinhibition in the rat. *Frontiers in systems neuroscience*, 7, 50.
- 423 Bubl, E., Perlov, E., & Tebartz Van Elst, L. (2006). Aripiprazole in patients with Tourette
424 syndrome. *The World Journal of Biological Psychiatry*, 7(2), 123-125.
- 425 Cavanna, A. E., Black, K. J., Hallett, M., & Voon, V. (2017). Neurobiology of the premonitory urge
426 in Tourette's syndrome: pathophysiology and treatment implications. *The Journal of*
427 *neuropsychiatry and clinical neurosciences*, 29(2), 95-104.

- 428 Conceição, V. A., Dias, Â., Farinha, A. C., & Maia, T. V. (2017). Premonitory urges and tics in
429 Tourette syndrome: computational mechanisms and neural correlates. *Current opinion in*
430 *neurobiology*, 46, 187-199.
- 431 Cox, J. H., Seri, S., & Cavanna, A. E. (2018). Sensory aspects of Tourette syndrome.
432 *Neuroscience & Biobehavioral Reviews*, 88, 170-176.
- 433 Draper, A., Jackson, G. M., Morgan, P. S., & Jackson, S. R. (2016). Premonitory urges are
434 associated with decreased grey matter thickness within the insula and sensorimotor
435 cortex in young people with Tourette syndrome. *Journal of Neuropsychology*, 10(1), 143-
436 153.
- 437 Eddy, C. M., Cavanna, A. E., Rickards, H. E., & Hansen, P. C. (2016). Temporo-parietal
438 dysfunction in Tourette syndrome: insights from an fMRI study of Theory of Mind. *Journal*
439 *of psychiatric research*, 81, 102-111.
- 440 Fahim, C., Yoon, U., Das, S., Lyttelton, O., Chen, J., Arnautelis, R., . . . Brandner, C. (2010).
441 Somatosensory–motor bodily representation cortical thinning in Tourette: Effects of tic
442 severity, age and gender. *Cortex*, 46(6), 750-760.
- 443 Fredericksen, K., Cutting, L., Kates, W., Mostofsky, S. H., Singer, H., Cooper, K., . . . Kaufmann,
444 W. E. (2002). Disproportionate increases of white matter in right frontal lobe in Tourette
445 syndrome. *Neurology*, 58(1), 85-89.
- 446 Ganos, C., Roessner, V., & Münchau, A. (2013). The functional anatomy of Gilles de la Tourette
447 syndrome. *Neuroscience & Biobehavioral Reviews*, 37(6), 1050-1062.
- 448 Greene, D. J., Church, J. A., Dosenbach, N. U., Nielsen, A. N., Adeyemo, B., Nardos, B., . . .
449 Schlaggar, B. L. (2016). Multivariate pattern classification of pediatric Tourette syndrome
450 using functional connectivity MRI. *Developmental science*, 19(4), 581-598.
- 451 Hammers, A., Allom, R., Koepp, M. J., Free, S. L., Myers, R., Lemieux, L., . . . Duncan, J. S.
452 (2003). Three-dimensional maximum probability atlas of the human brain, with particular
453 reference to the temporal lobe. *Human brain mapping*, 19(4), 224-247.

- 454 Handley, R., Zelaya, F. O., Reinders, A. S., Marques, T. R., Mehta, M. A., O'Gorman, R., . . .
455 Williams, S. (2013). Acute effects of single-dose aripiprazole and haloperidol on resting
456 cerebral blood flow (rCBF) in the human brain. *Human brain mapping, 34*(2), 272-282.
- 457 Hastie, T., Tibshirani, R., & Friedman, J. (2009). *The elements of statistical learning: data mining,*
458 *inference, and prediction*: Springer Science & Business Media.
- 459 Hirschtritt, M. E., Lee, P. C., Pauls, D. L., Dion, Y., Grados, M. A., Illmann, C., . . . Lyon, G. J.
460 (2015). Lifetime prevalence, age of risk, and genetic relationships of comorbid psychiatric
461 disorders in Tourette syndrome. *JAMA psychiatry, 72*(4), 325-333.
- 462 Jackson, S. R., Parkinson, A., Kim, S. Y., Schüermann, M., & Eickhoff, S. B. (2011). On the
463 functional anatomy of the urge-for-action. *Cognitive neuroscience, 2*(3-4), 227-243.
- 464 Jenkinson, M., Beckmann, C. F., Behrens, T. E., Woolrich, M. W., & Smith, S. M. (2012). Fsl.
465 *Neuroimage, 62*(2), 782-790.
- 466 Jordan, S., Koprivica, V., Dunn, R., Tottori, K., Kikuchi, T., & Altar, C. A. (2004). In vivo effects of
467 aripiprazole on cortical and striatal dopaminergic and serotonergic function. *European*
468 *journal of pharmacology, 483*(1), 45-53.
- 469 Kastrup, A., Schlotter, W., Plewnia, C., & Bartels, M. (2005). Treatment of tics in Tourette
470 syndrome with aripiprazole. *Journal of clinical psychopharmacology, 25*(1), 94-96.
- 471 Kates, W. R., Frederikse, M., Mostofsky, S. H., Folley, B. S., Cooper, K., Mazur-Hopkins, P., . . .
472 Pearlson, G. D. (2002). MRI parcellation of the frontal lobe in boys with attention deficit
473 hyperactivity disorder or Tourette syndrome. *Psychiatry Research: Neuroimaging, 116*(1-
474 2), 63-81.
- 475 Kundu, P., Inati, S. J., Evans, J. W., Luh, W.-M., & Bandettini, P. A. (2012). Differentiating BOLD
476 and non-BOLD signals in fMRI time series using multi-echo EPI. *Neuroimage, 60*(3),
477 1759-1770.
- 478 Kundu, P., Voon, V., Balchandani, P., Lombardo, M. V., Poser, B. A., & Bandettini, P. A. (2017).
479 Multi-echo fMRI: a review of applications in fMRI denoising and analysis of BOLD signals.
480 *Neuroimage, 154*, 59-80.

- 481 Leckman, J. F., Riddle, M. A., Hardin, M. T., Ort, S. I., Swartz, K. L., Stevenson, J., & Cohen, D.
482 J. (1989). The Yale Global Tic Severity Scale: initial testing of a clinician-rated scale of tic
483 severity. *Journal of the American Academy of Child & Adolescent Psychiatry*, 28(4), 566-
484 573.
- 485 Lee, W. H., & Frangou, S. (2017). Linking functional connectivity and dynamic properties of
486 resting-state networks. *Scientific reports*, 7(1), 1-10.
- 487 Lerner, A., Bagic, A., Boudreau, E., Hanakawa, T., Pagan, F., Mari, Z., . . . Simmons, J. (2007).
488 Neuroimaging of neuronal circuits involved in tic generation in patients with Tourette
489 syndrome. *Neurology*, 68(23), 1979-1987.
- 490 Lerner, A., Bagic, A., Hanakawa, T., Boudreau, E. A., Pagan, F., Mari, Z., . . . Murphy, D. L.
491 (2009). Involvement of insula and cingulate cortices in control and suppression of natural
492 urges. *Cerebral cortex*, 19(1), 218-223.
- 493 Marques, J. Retrieved from <https://github.com/JosePMarques/MP2RAGE-related-scripts>
- 494 Martino, D., Ganos, C., & Worbe, Y. (2018). Neuroimaging applications in Tourette's syndrome.
495 *International review of neurobiology*, 143, 65-108.
- 496 Mazzone, L., Yu, S., Blair, C., Gunter, B. C., Wang, Z., Marsh, R., & Peterson, B. S. (2010). An
497 fMRI study of frontostriatal circuits during the inhibition of eye blinking in persons with
498 Tourette syndrome. *American Journal of Psychiatry*, 167(3), 341-349.
- 499 McCairn, K. W., Iriki, A., & Isoda, M. (2013). Global dysrhythmia of cerebro-basal ganglia–
500 cerebellar networks underlies motor tics following striatal disinhibition. *Journal of*
501 *Neuroscience*, 33(2), 697-708.
- 502 Mostofsky, S. H., Schafer, J. G., Abrams, M. T., Goldberg, M. C., Flower, A. A., Boyce, A., . . .
503 Denckla, M. B. (2003). fMRI evidence that the neural basis of response inhibition is task-
504 dependent. *Cognitive brain research*, 17(2), 419-430.
- 505 Nielsen, A. N., Barch, D. M., Petersen, S. E., Schlaggar, B. L., & Greene, D. J. (2019). Machine
506 learning with neuroimaging: evaluating its applications in psychiatry. *Biological*
507 *Psychiatry: Cognitive Neuroscience and Neuroimaging*.

- 508 Nielsen, A. N., Gratton, C., Church, J. A., Dosenbach, N. U., Black, K. J., Petersen, S. E., . . .
509 Greene, D. J. (2020). Atypical functional connectivity in Tourette syndrome differs
510 between children and adults. *Biological psychiatry*, *87*(2), 164-173.
- 511 O'Brien, K. R., Kober, T., Hagmann, P., Maeder, P., Marques, J., Lazeyras, F., . . . Roche, A.
512 (2014). Robust T1-weighted structural brain imaging and morphometry at 7T using
513 MP2RAGE. *PloS one*, *9*(6).
- 514 Power, J. D., Mitra, A., Laumann, T. O., Snyder, A. Z., Schlaggar, B. L., & Petersen, S. E. (2014).
515 Methods to detect, characterize, and remove motion artifact in resting state fMRI.
516 *Neuroimage*, *84*, 320-341.
- 517 Rae, C. L., Critchley, H. D., & Seth, A. K. (2019). A Bayesian account of the sensory-motor
518 interactions underlying symptoms of Tourette syndrome. *Frontiers in psychiatry*, *10*, 29.
- 519 Ramkiran, S., Heidemeyer, L., Gaebler, A., Shah, N. J., & Neuner, I. (2019). Alterations in basal
520 ganglia-cerebello-thalamo-cortical connectivity and whole brain functional network
521 topology in Tourette's syndrome. *NeuroImage: Clinical*, *24*, 101998.
- 522 Richiardi, J., Gschwind, M., Simioni, S., Annoni, J.-M., Greco, B., Hagmann, P., . . . Van De Ville,
523 D. (2012). Classifying minimally disabled multiple sclerosis patients from resting state
524 functional connectivity. *Neuroimage*, *62*(3), 2021-2033.
- 525 Shirer, W. R., Ryali, S., Rykhlevskaia, E., Menon, V., & Greicius, M. D. (2012). Decoding subject-
526 driven cognitive states with whole-brain connectivity patterns. *Cerebral cortex*, *22*(1), 158-
527 165.
- 528 Sigurdsson, H. P., Jackson, S. R., Jolley, L., Mitchell, E., & Jackson, G. M. (2020). Alterations in
529 cerebellar grey matter structure and covariance networks in young people with Tourette
530 syndrome. *Cortex*, *126*, 1-15.
- 531 Singer, H. S. (2005). Tourette's syndrome: from behaviour to biology. *The Lancet Neurology*, *4*(3),
532 149-159.
- 533 Tinaz, S., Malone, P., Hallett, M., & Horovitz, S. G. (2015). Role of the right dorsal anterior insula
534 in the urge to tic in Tourette syndrome. *Movement Disorders*, *30*(9), 1190-1197.

- 535 Tzourio-Mazoyer, N., Landeau, B., Papathanassiou, D., Crivello, F., Etard, O., Delcroix, N., . . .
536 Joliot, M. (2002). Automated anatomical labeling of activations in SPM using a
537 macroscopic anatomical parcellation of the MNI MRI single-subject brain. *Neuroimage*,
538 *15*(1), 273-289.
- 539 Wegrzyk, J., Kebets, V., Richiardi, J., Galli, S., Van de Ville, D., & Aybek, S. (2018). Identifying
540 motor functional neurological disorder using resting-state functional connectivity.
541 *NeuroImage: Clinical*, *17*, 163-168.
- 542 Wolfers, T., Buitelaar, J. K., Beckmann, C. F., Franke, B., & Marquand, A. F. (2015). From
543 estimating activation locality to predicting disorder: a review of pattern recognition for
544 neuroimaging-based psychiatric diagnostics. *Neuroscience & Biobehavioral Reviews*, *57*,
545 328-349.
- 546 Worbe, Y., Gerardin, E., Hartmann, A., Valabrégue, R., Chupin, M., Tremblay, L., . . . Lehericy, S.
547 (2010). Distinct structural changes underpin clinical phenotypes in patients with Gilles de
548 la Tourette syndrome. *Brain*, *133*(12), 3649-3660.
- 549 Worbe, Y., Lehericy, S., & Hartmann, A. (2015). Neuroimaging of tic genesis: present status and
550 future perspectives. *Movement Disorders*, *30*(9), 1179-1183.
- 551 Worbe, Y., Malherbe, C., Hartmann, A., Péligrini-Issac, M., Messé, A., Vidailhet, M., . . . Benali,
552 H. (2012). Functional immaturity of cortico-basal ganglia networks in Gilles de la Tourette
553 syndrome. *Brain*, *135*(6), 1937-1946.
- 554 Worbe, Y., Sgambato-Faure, V., Epinat, J., Chaigneau, M., Tandé, D., François, C., . . .
555 Tremblay, L. (2013). Towards a primate model of Gilles de la Tourette syndrome:
556 anatomo-behavioural correlation of disorders induced by striatal dysfunction. *Cortex*,
557 *49*(4), 1126-1140.
- 558 Wu, G., & Chang, E. Y. (2003). *Class-boundary alignment for imbalanced dataset learning*. Paper
559 presented at the ICML 2003 workshop on learning from imbalanced data sets II,
560 Washington, DC.
- 561

562 TABLES

563 **Table 1. Clinical and demographic data.** Comparison of clinical and demographic scores across
 564 groups. YGTSS=Yale global tic severity score; IED=intermittent explosive disorder;
 565 ADHD=attention deficit hyperactivity disorder; OCD=obsessive compulsive disorder; HC=healthy
 566 controls; TD=Tourette disorder.

	HC (N = 51)	TD (N = 48)	Statistics	TD without medication (N = 18)	TD with medication (N = 18)	Statistics
Sex			$\chi(1) =$			$\chi(1) =$
[male / female]	33 / 18	38 / 10	2.55, p = 0.110	14 / 4	13 / 5	0.15, p = 0.700
Age			t(97) =			t(34) =
[years, mean \pm SD]	30.9 \pm 10.4	30.5 \pm 10.3	2.11, p = 0.833	30.7 \pm 11.2	31.4 \pm 9.5	0.21, p = 0.836
YGTSS50	-	16.5 \pm 7.2	-	15.5 \pm 8.0	17.11 \pm 6.0	t(34) = 0.68, p = 0.498
IED [N (% of TD)]	-	22 (45.8%)	-	50%	38.9%	$\chi(1) =$ 0.45, p = 0.502
ADHD [N (% of TD)]	-	20 (41.7%)	-	38.9%	27.8%	$\chi(1) =$ 0.50, p = 0.480
OCD [N (% of TD)]	-	10 (20.8%)	-	11.1%	16.7%	$\chi(1) =$ 0.23, p = 0.630

Overall medication [N (% of TD)]*	-	18 (37.5%)		
- Aripiprazole, APZ [N (% of TD)]	-	15 (31.2%)		
- Topiramate [N (% of TD)]	-	2 (4.2%)		
- Fluoxetine [N (% of TD)]	-	2 (4.2%)		
- Risperidone [N (% of TD)]	-	2 (4.2%)		
- Others (Pimozide, Escitalopram, Haloperidol, Mianserin –)	-	4 (8.3%)		

567 * all medications were prescribed for at least three years.

568

569

570

571 **Table 2. Results of the multivariate analysis.** Predictive performance of the Support Vector
 572 Machine Classifiers. P-values represent the significance of the results, compared to chance.
 573 HC=healthy controls; TD=Tourette disorder

	Accuracy (%)	Specificity (%)	Sensitivity (%)	p-value
Between-group classifier (TD vs HC)	67	65	69	0.004
Between-TD patients' subgroup classifier (TD with vs without medication)	69	67	72	0.019

574

575

576

577

578

579

580

581

582

583

584

585

586

587

588

589

590

591 **FIGURE LEGENDS**

592 **Figure 1. SVM classifier with all HC and patients, most discriminative connections.** Color
593 code represents the absolute weights assigned to the connections. Node size represents the
594 mean weighted number of connections entering the node over the entire set of 6670 weights. Line
595 thickness represents the absolute mean weight of the connection over the entire set. For
596 graphical purposes, the figure is truncated so that only the top 30 connections are displayed. (A)
597 SVM for TD vs. HC. (B) SVM for medicated vs. unmedicated TD. R=right; L=left; Ang=Angular
598 gyrus; Caud=nucleus caudate; Cereb(N)=Nth cerebellar lobule; Ins=insula; medSFG=medial
599 segment of the superior frontal gyrus; PCL=paracentral lobule; Put=putamen; REC=rectus gyrus;
600 SMA=supplementary motor area; SMG=supramarginal gyrus; SPG=superior parietal gyrus;
601 supORB=superior segment of the orbital gyrus; Thal=thalamus; triangIFG=pars triangularis of the
602 inferior frontal gyrus.

603

604

605

606

607

608

609

610

611

612

613

614

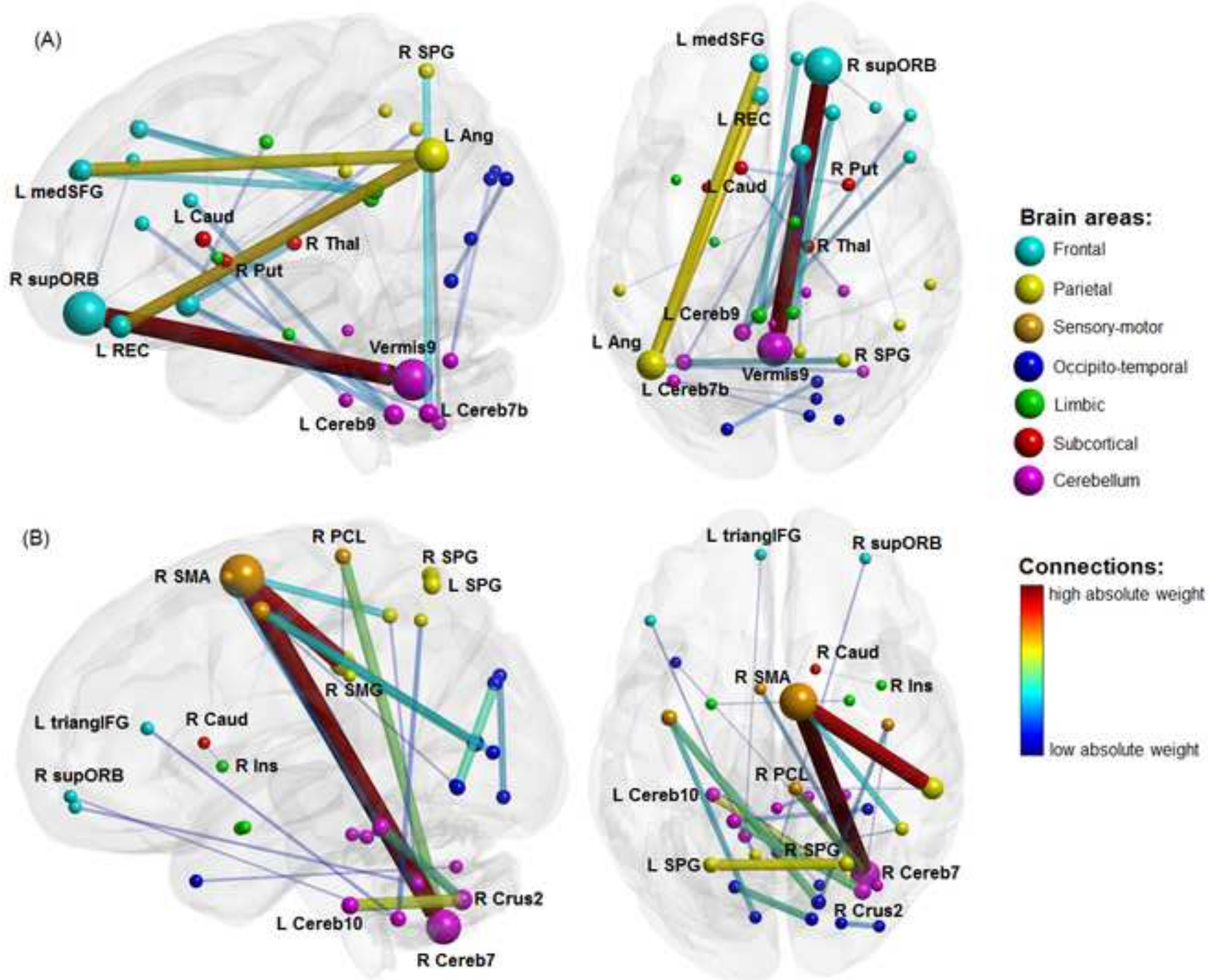
615

616

617

618

619 **Figure 2. Results of the univariate analysis.** (A) Functional connectivity between TD and HC.
620 (B) Functional connectivity between medicated and unmedicated TD. Bars represent the mean
621 values \pm SE of the mean. * depicts significant differences at independent-sample t-tests.



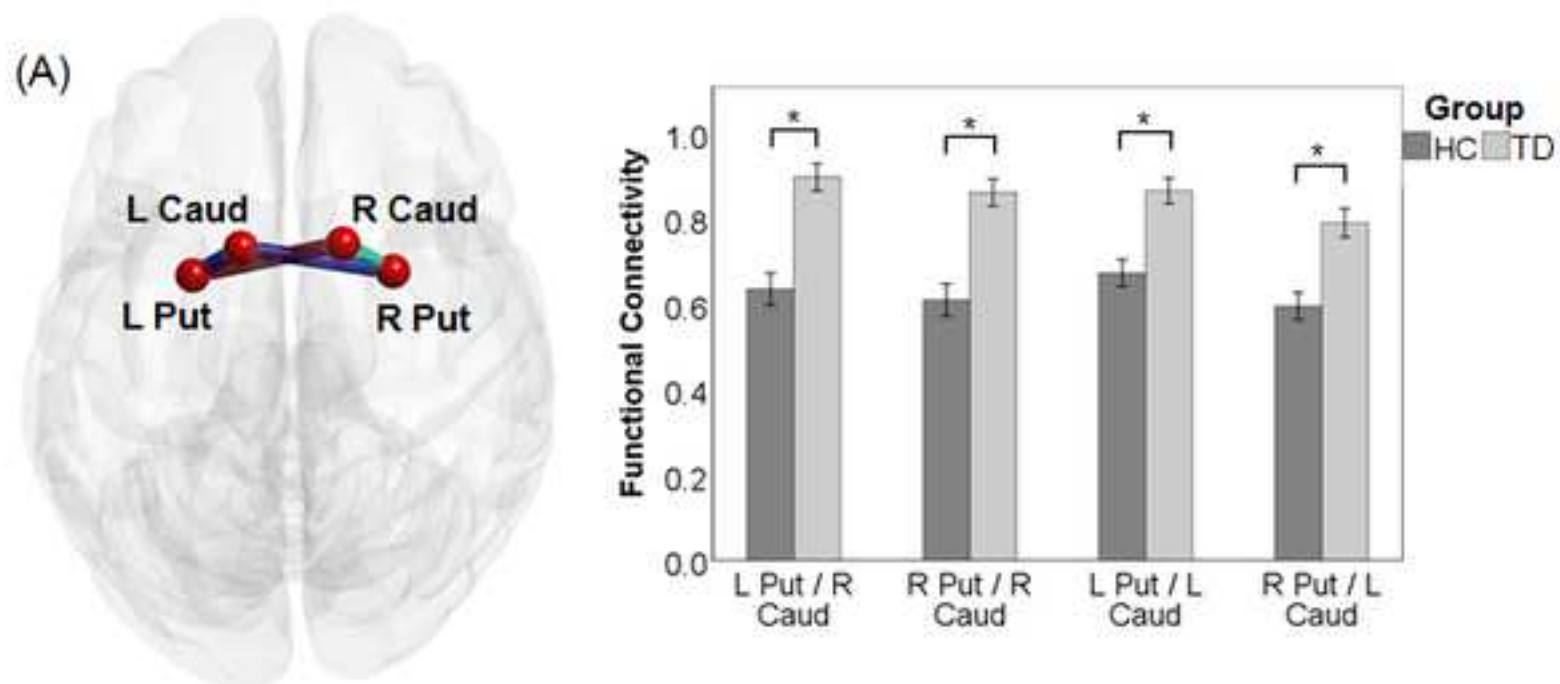
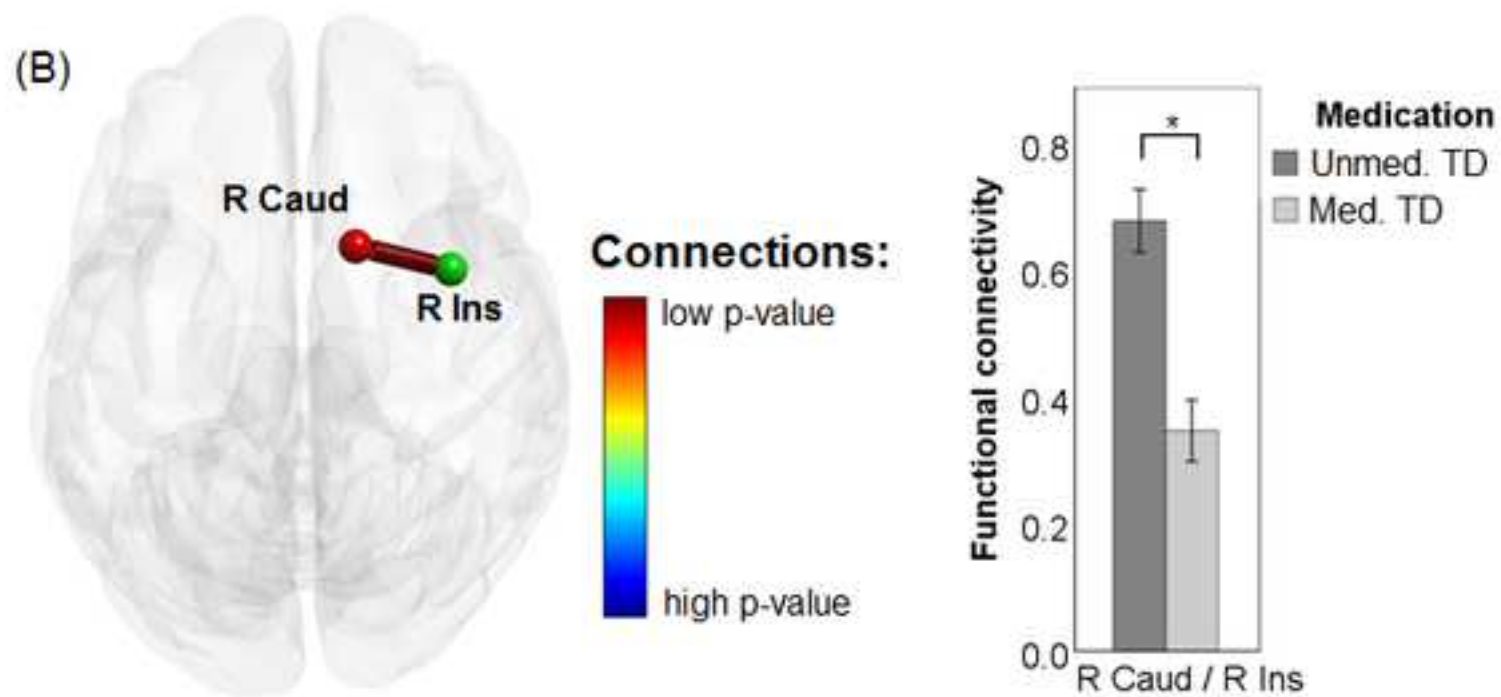
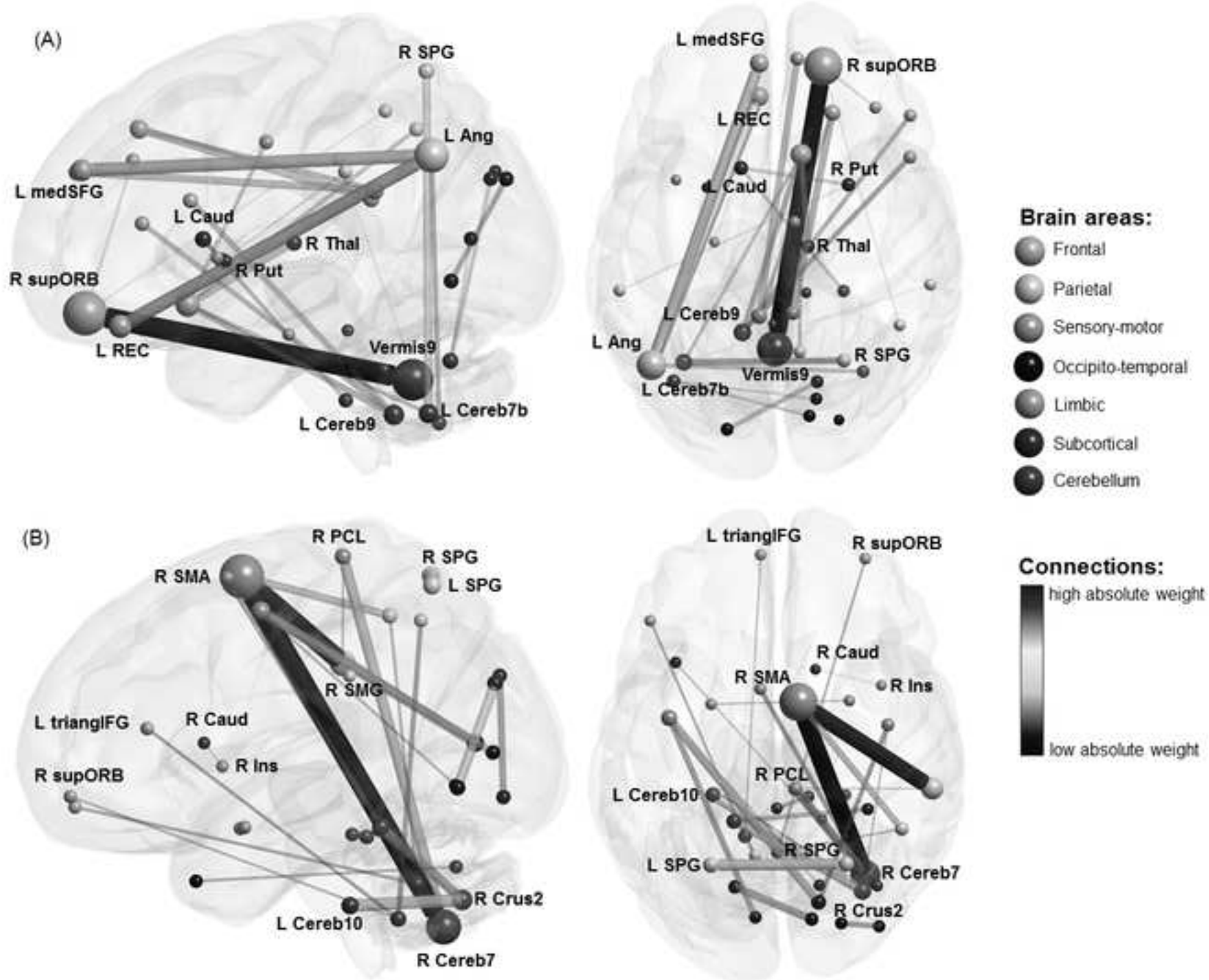


Figure2_color.tif





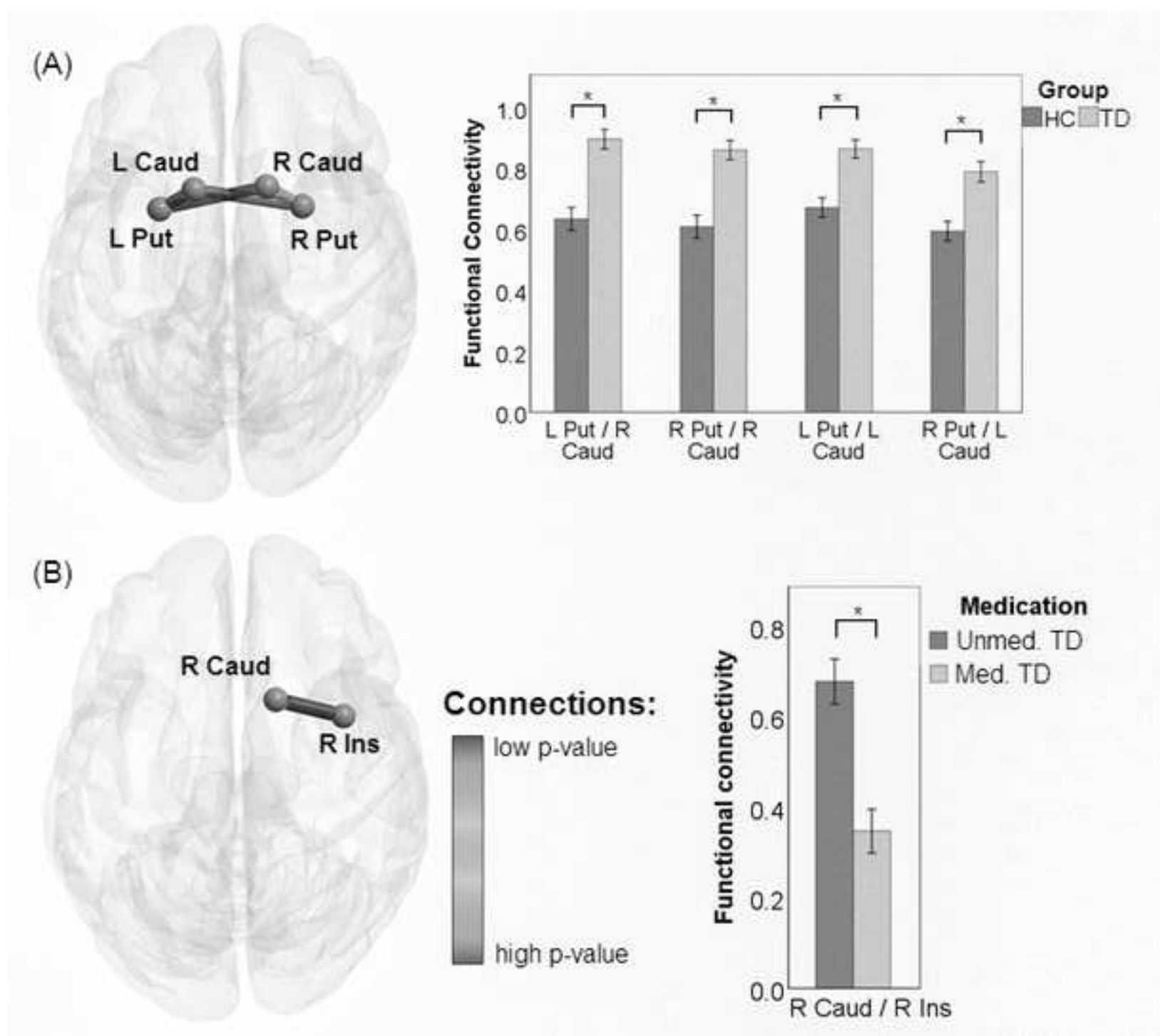


Figure2_color.tif

Table 1. Clinical and demographic data. Comparison of clinical and demographic scores across groups. YGTSS=Yale global tic severity score; IED=intermittent explosive disorder; ADHD=attention deficit hyperactivity disorder; OCD=obsessive compulsive disorder; HC=healthy controls; TD=Tourette disorder.

	HC (N = 51)	TD (N = 48)	Statistics	TD without medication (N = 18)	TD with medication (N = 18)	Statistics
Sex [male / female]	33 / 18	38 / 10	$\chi(1) =$ 2.55, p = 0.110	14 / 4	13 / 5	$\chi(1) =$ 0.15, p = 0.700
Age [years, mean \pm SD]	30.9 \pm 10.4	30.5 \pm 10.3	t(97) = 2.11, p = 0.833	30.7 \pm 11.2	31.4 \pm 9.5	t(34) = 0.21, p = 0.836
YGTSS50	-	16.5 \pm 7.2	-	15.5 \pm 8.0	17.11 \pm 6.0	t(34) = 0.68, p = 0.498
IED [N (% of TD)]	-	22 (45.8%)	-	50%	38.9%	$\chi(1) =$ 0.45, p = 0.502
ADHD [N (% of TD)]	-	20 (41.7%)	-	38.9%	27.8%	$\chi(1) =$ 0.50, p = 0.480
OCD [N (% of TD)]	-	10 (20.8%)	-	11.1%	16.7%	$\chi(1) =$ 0.23, p = 0.630
Overall medication [N (% of TD)]*	-	18 (37.5%)				

-			
Aripiprazole, APZ [N (% of TD)]	-	15 (31.2%)	
- Topiramate [N (% of TD)]	-	2 (4.2%)	
- Fluoxetine [N (% of TD)]	-	2 (4.2%)	
- Risperidone [N (% of TD)]	-	2 (4.2%)	
- Others (Pimozide, Escitalopram, Haloperidol, Mianserin – [N (% of TD)])	-	4 (8.3%)	

* all medications were prescribed for at least three years.

Table 2. Results of the multivariate analysis. Predictive performance of the Support Vector Machine Classifiers. P-values represent the significance of the results, compared to chance. HC=healthy controls; TD=Tourette disorder

	Accuracy (%)	Specificity (%)	Sensitivity (%)	p-value
Between-group classifier (TD vs HC)	67	65	69	0.004
Between-TD patients' subgroup classifier (TD with vs without medication)	69	67	72	0.019